Cell

The RIDDLE Syndrome Protein Mediates a Ubiquitin-Dependent Signaling Cascade at Sites of DNA Damage

Grant S. Stewart,[1,5,*] Stephanie Panier,[2,3,5] Kelly Townsend,[1] Abdallah K. Al-Hakim,[2] Nadine K. Kolas,[2] Edward S. Miller,[1] Shinichiro Nakada,[2] Jarkko Ylanko,[2,3] Signe Olivarius,[2] Megan Mendez,[2] Ceri Oldreive,[1] Jan Wildenhain,[2] Andrea Tagliaferro,[2] Laurence Pelletier,[2,3] Nadine Taubenheim,[4] Anne Durandy,[4] Philip J. Byrd,[1] Tatjana Stankovic,[1] A. Malcolm R. Taylor,[1] and Daniel Durocher[2,3,*]

[1]Cancer Research UK, Institute for Cancer Studies, University of Birmingham, Vincent Drive, Edgbaston, Birmingham B15 2TT, UK

[2]Samuel Lunenfeld Research Institute, Mount Sinai Hospital, 600 University Avenue, Toronto, M5G 1X5 Ontario, Canada

[3]Department of Molecular Genetics, University of Toronto, Toronto, M5S 1A8 Ontario, Canada

[4]INSERM U768, Hopital Necker-Enfants Malades, 149 Rue de Sevres, 75015 Paris, France

[5]These authors contributed equally to this work

*Correspondence: g.s.stewart@bham.ac.uk (G.S.S.), durocher@lunenfeld.ca (D.D.)

DOI 10.1016/j.cell.2008.12.042

SUMMARY

The biological response to DNA double-strand breaks acts to preserve genome integrity. Individuals bearing inactivating mutations in components of this response exhibit clinical symptoms that include cellular radiosensitivity, immunodeficiency, and cancer predisposition. The archetype for such disorders is Ataxia-Telangiectasia caused by biallelic mutation in *ATM*, a central component of the DNA damage response. Here, we report that the ubiquitin ligase RNF168 is mutated in the RIDDLE syndrome, a recently discovered immunodeficiency and radiosensitivity disorder. We show that RNF168 is recruited to sites of DNA damage by binding to ubiquitylated histone H2A. RNF168 acts with UBC13 to amplify the RNF8-dependent histone ubiquitylation by targeting H2A-type histones and by promoting the formation of lysine 63-linked ubiquitin conjugates. These RNF168-dependent chromatin modifications orchestrate the accumulation of 53BP1 and BRCA1 to DNA lesions, and their loss is the likely cause of the cellular and developmental phenotypes associated with RIDDLE syndrome.

INTRODUCTION

DNA damage, signaling, and repair are fundamental processes required to maintain cellular viability and homeostasis. Among the different types of DNA lesions, the DNA double-strand break (DSB) is considered the most harmful. Indeed, unrepaired DSBs can be lethal to the cell, and their inaccurate repair leads to chromosomal rearrangements that promote tumorigenesis (Jeggo and Lobrich, 2007). Defects in DSB repair are also associated with accelerated aging, exhaustion of stem cell pools, infertility, and impaired development of the nervous and immune systems (Callen et al., 2007; McKinnon and Caldecott, 2007). Therefore, to counteract these unwanted outcomes, DSBs elicit a complex response that promotes DNA repair and profoundly influences multiple aspects of cellular physiology (Jeggo and Lobrich, 2007).

Germline mutations in genes coding for regulators of the DSB response are responsible for complex diseases that have a wide range of clinical phenotypes. A paradigm for such syndromes is Ataxia-Telangiectasia (A-T) caused by biallelic mutations in *ATM*, which encodes a serine/threonine kinase of the PI(3) kinase-like kinases family (Savitsky et al., 1995). Loss of ATM results in progressive neurodegeneration, immune dysfunction, hypersensitivity to ionizing radiation (IR), and marked predisposition to cancer (Lavin and Shiloh, 1997). At the cellular level, ATM is at the hub of the response to DSBs. ATM rapidly accumulates at DNA lesions in a MRE11/RAD50/NBS1 (MRN)-dependent manner to initiate a cascade of protein recruitment at sites of DNA damage (Bekker-Jensen et al., 2006). This chromatin-based cascade promotes DNA repair and activation of cell-cycle checkpoints, two critical outcomes of the DNA damage response. The accumulation of proteins at DSB sites produces characteristic subnuclear foci that are easily visualized by fluorescence microscopy.

ATM promotes the relocalization of many repair and signaling proteins at DNA breaks largely via the phosphorylation of the histone H2A variant H2AX on Ser139 (Rogakou et al., 1998; Stiff et al., 2004). H2AX phosphorylation (referred to as γ-H2AX) establishes a chromatin domain onto which regulators of the DSB response accumulate. In particular, the γ-H2AX phosphoepitope is directly recognized by the BRCT domains of the mediator protein MDC1 (Lou et al., 2006; Stewart et al., 2003; Stucki et al., 2005). MDC1 acts as a molecular scaffold that stabilizes the MRN complex bound to damaged chromatin while promoting further accumulation of MRN and activated ATM. MDC1, therefore, amplifies the ATM-dependent DNA damage response (Lou et al., 2006; Stucki et al., 2005).

MDC1 is also phosphorylated by ATM on "TQXF" motifs (Huen et al., 2007; Kolas et al., 2007; Matsuoka et al., 2007) that promote the recruitment of RNF8, an E3 ubiquitin ligase (Huen et al., 2007; Kolas et al., 2007; Mailand et al., 2007; Plans et al., 2006). RNF8, in turn, independently stimulates the

recruitment of the RAP80-ABRA1-BRCA1 complex and the accumulation of 53BP1 at sites of DNA damage (Huen et al., 2007; Kolas et al., 2007; Mailand et al., 2007; Sakasai and Tibbetts, 2008; Wang and Elledge, 2007). RNF8 most likely facilitates the relocalization of these repair proteins by catalyzing the ubiquitylation of H2A-type histones surrounding the DNA lesion (Huen et al., 2007; Mailand et al., 2007). Because the ubiquitin-binding motifs of RAP80 (UIMs) mediate BRCA1 recruitment to sites of DNA lesions, it is likely that RAP80 directly binds the products of RNF8 ubiquitylation to facilitate BRCA1-dependent DSB repair. By contrast, 53BP1 does not possess ubiquitin-binding domains, and its localization to DNA damage sites, rather, depends on its Tudor domain, a methyl-lysine residue-binding module (Botuyan et al., 2006; Huyen et al., 2004). It is, therefore, possible that modification of chromatin by RNF8 enables the recognition of methylated histones by the 53BP1 Tudor domain. The precise function of 53BP1 and its role during the cellular response to DNA damage is unclear, although it has been implicated in regulating the G2/M phase checkpoint (DiTullio et al., 2002; Wang et al., 2002) class switch recombination (CSR) (Manis et al., 2004) as well as repair of DNA DSBs via nonhomologous end-joining (NHEJ) (Difilippantonio et al., 2008).

Recently, RIDDLE (radiosensitivity, immunodeficiency, dysmorphic features, and learning difficulties) syndrome, a novel human immunodeficiency disorder associated with defective DSB repair, has been described (Stewart et al., 2007). RIDDLE syndrome shares overlapping clinical features with A-T, and cells derived from a RIDDLE patient (15-9BI) exhibit impaired relocalization of 53BP1 and BRCA1 to DSBs, while MDC1 and NBS1 remain unaffected (Stewart et al., 2007). However, efforts to identify the gene responsible for this disorder have so far failed, suggesting that a novel participant of the DNA damage response is responsible for this syndrome.

Here, we report the identification of the gene mutated in RIDDLE syndrome, *RNF168*, by mining an RNA interference screen that examined 53BP1 focal accumulation at sites of DNA damage. RNF168 itself accumulates at DSBs downstream of RNF8 through a physical interaction with ubiquitylated H2A. Like RNF8, RNF168 is also an E3 ubiquitin ligase that acts in concert with UBC13 to catalyze the formation of lysine 63 (K63)-linked ubiquitin conjugates and promotes the ubiquitylation of H2A-type histones surrounding the damage, thereby amplifying, or spreading, the regulatory ubiquitylation signal initiated by RNF8. In turn, RNF168-dependent ubiquitylation mediates the accumulation of 53BP1 and BRCA1 at DNA lesions to promote DSB repair, DNA damage checkpoints, and survival following IR exposure. Our results, therefore, indicate that the protein ubiquitylation cascade controlled by RNF8 and RNF168 is a physiologically important response to DSBs in human cells and suggest that the RNF8/RNF168 pathway might be an important conduit for ATM-dependent DNA damage signaling.

RESULTS

RNF168 Promotes the Accumulation of 53BP1 and BRCA1 at Sites of DNA Damage

A hallmark of RIDDLE cells is the inability of 53BP1 to relocalize to sites of DNA double-strand breaks (Stewart et al., 2007). In the absence of any detectable mutations in either *RNF8* or *UBC13* in these cells (G.S.S., unpublished data), we reasoned that any new gene necessary for 53BP1 focus formation would be an ideal candidate for being mutated in the RIDDLE syndrome. Therefore, we mined a siRNA screen that utilized 53BP1 focus formation as a readout (Figure S1 available online) (Kolas et al., 2007). From the initial screen, we narrowed down our search to a set of 59 candidate genes that displayed a statistical reduction in 53BP1 focus formation 24 hr postirradiation (Table S1). The contribution of each of these genes for the accumulation of 53BP1 at sites of DNA damage was directly tested in a secondary screen. HeLa cells grown in 384-well plates were transfected with enzymatically prepared siRNA (esiRNA), as described previously (Kolas et al., 2007), and fixed 1 hr postirradiation before being processed for 53BP1 immunofluorescence and automated microscopy. The knockdown of RNF8 was used as a positive control, and an esiRNA-targeting firefly luciferase was used as a negative control. As shown in Figure 1A, the esiRNA-targeting RNF168 and ubiquitin (UBB) yielded a reduction in 53BP1 foci that approached that of RNF8 depletion. Given that ubiquitin mutations were unlikely to cause RIDDLE syndrome, we focused our attention on RNF168. To confirm that the impairment of 53BP1 localization to sites of DNA damage was, indeed, caused by depletion of the RNF168 protein, we rescued the 53BP1 foci phenotype by reintroduction of a siRNA-resistant epitope-tagged RNF168 cDNA (RNF168*) (Figure 1B). Then, we raised a polyclonal antibody against RNF168 that confirmed that both the esiRNA and siRNA against RNF168 efficiently knocked down protein expression (Figures 1C and S1E). From these results, we concluded that RNF168 is critical for the accumulation, or retention, of 53BP1 at sites of DNA damage in response to IR.

Next, we addressed whether RNF168 is involved in the formation of BRCA1, NBS1, γ-H2AX, MDC1, RIF1, and conjugated ubiquitin foci after IR, following the siRNA-mediated depletion of RNF168 in U2OS cells. We found that, in addition to promoting 53BP1 focus formation, RNF168 also promotes the accumulation of BRCA1 and RIF1 at sites of DNA damage (Figures 1D and S2). Moreover, RNF168 depletion severely impaired the formation of conjugated ubiquitin foci as detected by the FK2 monoclonal antibody (Figures 1D and S2). In contrast, RNF168 depletion by RNAi did not adversely affect the formation of γ-H2AX, MDC1, and NBS1 IR-induced foci (Figures 1D and S2). Therefore, we concluded that RNF168 plays an important role in the ubiquitylation pathway that mediates 53BP1 and BRCA1 recruitment to sites of DNA damage downstream of MDC1. Importantly, the phenotypes imparted by RNF168 depletion overlap with those observed in cells derived from the 15-9BI RIDDLE patient. *RNF168* was, therefore, considered as a prime candidate for the gene mutated in the RIDDLE syndrome.

Biallelic Mutations in *RNF168* Cause RIDDLE Syndrome

To look for *RNF168* mutations in 15-9BI RIDDLE cells, we amplified and sequenced the *RNF168* exons from genomic DNA (Figure 2A). Two mutations were identified. The first mutation was a duplication of a G nucleotide at position 397 (*c.397 dupG*). This insertion produces a frameshifted mRNA that codes for a protein that contains the first 132 amino acid residues of the wild-type protein followed by 12 residues coded by the shifted

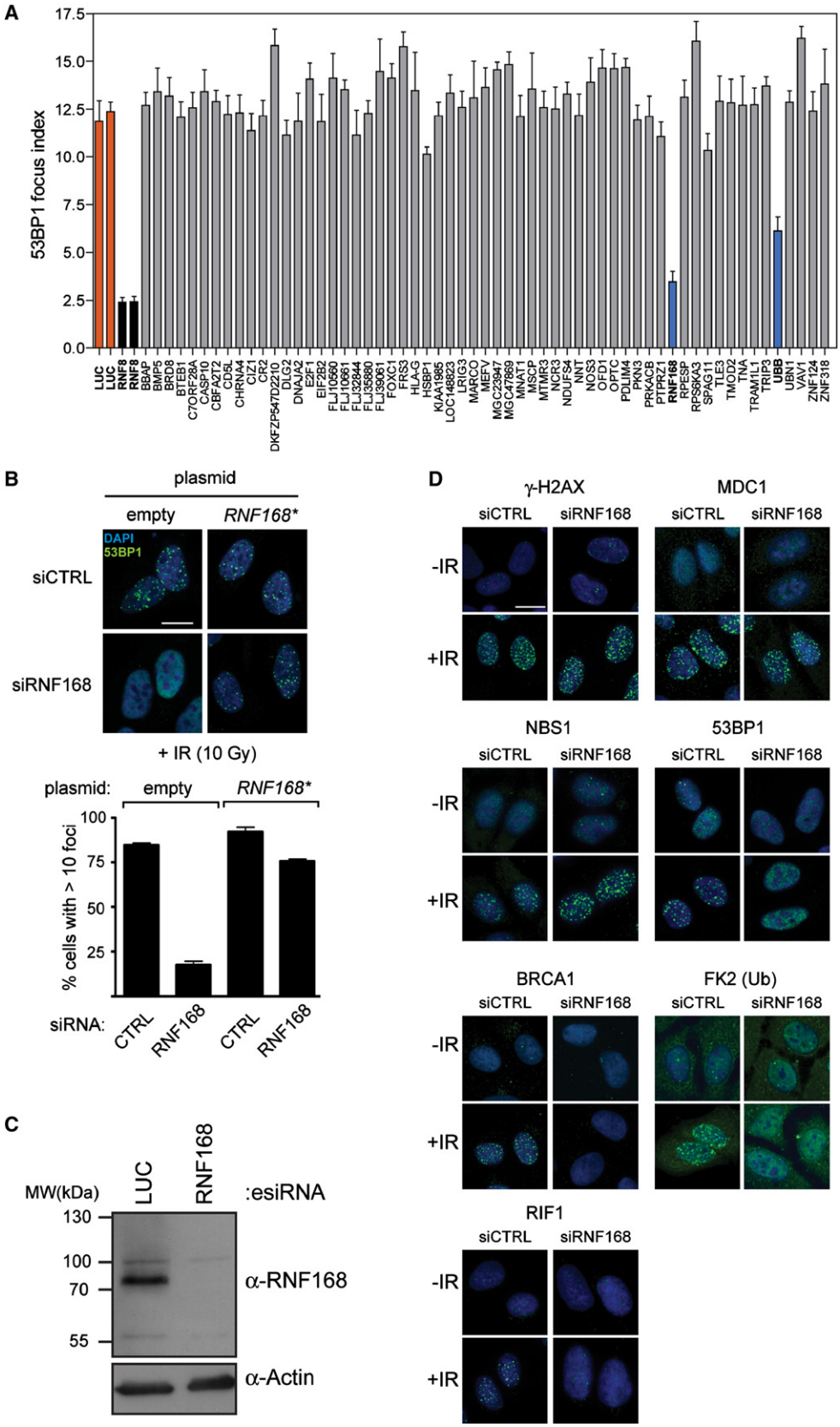
A
53BP1 focus index
17.5
15.0
12.5
10.0
7.5
5.0
2.5
0.0
LUC
LUC
RNF8
RNF8
BBAP
BMP5
BRD8
BTEB1
C7ORF28A
CAST10
CBFA2T2
CD72
CHRNA4
CIZ1
CR2
DKFZP547D2210
DLG2
DNAJA2
E2F1
EIF2B2
FLJ10560
FLJ10661
FLJ32844
FLJ35880
FLJ39061
FOXC1
FRS3
HLA-G
HSBP1
KIAA1985
LOC148823
LRIG3
MARCO
MEFV
MGC23947
MGC47869
MNAT1
MSCP
MTMR3
NCR3
NDUFS4
NNT
NOS3
OFD1
OPTC
PDLIM4
PKN3
PRKAC2B
PTPRZ1
RNF168
RPE3P
RPS6KA3
SPAG11
TLE3
TMOD2
TNA
TRAM1L1
TRIP3
UBB
UBN1
VAV1
ZNF124
ZNF318
B
plasmid
empty
RNF168*
DAPI
53BP1
siCTRL
siRNF168
+ IR (10 Gy)
plasmid:
empty
RNF168*
% cells with > 10 foci
100
75
50
25
siRNA:
CTRL
RNF168
CTRL
RNF168
C
MW(kDa)
LUC
RNF168
:esiRNA
130
100
70
55
α-RNF168
α-Actin
D
γ-H2AX
MDC1
siCTRL
siRNF168
siCTRL
siRNF168
-IR
+IR
NBS1
53BP1
siCTRL
siRNF168
siCTRL
siRNF168
-IR
+IR
BRCA1
FK2 (Ub)
siCTRL
siRNF168
siCTRL
siRNF168
-IR
+IR
RIF1
siCTRL
siRNF168
-IR
+IR

reading frame (p.Ala133GlyfsX11; A133fsX in short) (Figure 2B). The second mutation was a deletion of nucleotides 1323–1326 (*c.1323_1326 delACAA*) leading to a predicted protein that contains the first 441 wild-type residues of RNF168 followed by 46 amino acid residues resulting from the shifted reading frame (p.Gln442LysfsX45, referred to hereafter as Q442fsX) (Figure 2B). Moreover, sequencing *RNF168* in the parents of 15-9BI indicated that the *c.397 dupG* mutation originated from the father, whereas the *c.1323_1326 delACAA* mutation was transmitted by the mother (Figure 2A). The 15-9BI patient, therefore, contains biallelic mutations in the *RNF168* gene, which are predicted to result in aberrant RNF168 proteins. These results strongly suggest that RIDDLE is a recessive disorder.

To determine whether the mutant RNF168 proteins are expressed in RIDDLE cells, we generated an additional antibody directed against the N-terminal region of RNF168. This antibody detects endogenous RNF168 after immunoprecipitation (Figure S3) and was used to immunoprecipitate RNF168 from BJ human fibroblasts, RIDDLE 15-9BI cells, and 15-9BI cells stably expressing wild-type RNF168. While we readily detected RNF168 in BJ and 15-9BI cells expressing RNF168, in the 15-9BI cells, we failed to detect any band that would correspond to the A133fsX or Q442fsX mutant proteins (Figure 2C). These results indicate that, in cells derived from the 15-9BI patient, the RNF168 mutant proteins, if expressed at all, are grossly underexpressed relative to normal levels.

Analysis of the predicted RNF168 protein sequence suggested that RNF168 might be an E3 ubiquitin ligase by virtue of its N-terminal RING finger motif (Figure 2B). Furthermore, RNF168 contains two ubiquitin interaction motifs, termed MIU for "motif interacting with ubiquitin," that have been shown to selectively bind to ubiquitin chains (Penengo et al., 2006). Interestingly, neither *RNF168* mutations found in the 15-9BI patient affect the RING finger motif, but both result in predicted proteins that either lack a single (Q442fsX) or both (A133fsX) MIU motifs (Figure 2B).

To ascertain whether the *RNF168* gene is responsible for the cellular phenotypes associated with RIDDLE syndrome, we introduced wild-type *RNF168* tagged with hemagglutinin (HA) into 15-9BI fibroblasts via retroviral transduction (Figure 2D). Two independent clones were selected, and their clonogenic survival in response to IR was determined. As shown in Figure 2E, wild-type *HA-RNF168* restores radio resistance to the 15-9BI fibroblasts. In addition, the *HA-RNF168*-complemented cells became proficient in the accumulation of BRCA1, 53BP1, RAP80, and ubiquitin conjugates at sites of DNA damage (Figures 2F and S4). Together, these data indicate that recessive mutations in the *RNF168* gene are responsible for the cellular defects observed in the 15-9BI patient.

DNA Damage Signaling by RNF168 Requires Its RING and MIU Domains

The presence of a RING finger in RNF168 along with the two MIU motifs suggests that its putative E3 ligase activity, or its ability to bind ubiquitin, might be important for its function in the DNA damage response. To map the functionally relevant regions of RNF168, we generated a set of HCT116 cell lines that express siRNA-resistant *RNF168* (wild-type or mutant) under the control of a tetracycline-inducible promoter. First, we deleted the RING finger (ΔRING) to examine the contribution of the potential E3 ligase activity of RNF168 since point mutations in the RING finger motif resulted in proteins that were poorly expressed (data not shown). To assess the contribution of the MIU motifs, we introduced mutations that impair but do not totally abolish ubiquitin binding (Penengo et al., 2006) singly or in combination (yielding the A179G, A450G, and A179/A450G mutants). In addition, we also excised the entire MIU motifs singly or in combination (yielding the ΔMIU1, ΔMIU2, and ΔMIU1/2 mutants). Addition of tetracycline (tet) to the media for 24 hr resulted in exogenous protein expression that was roughly 3- to 5-fold higher than that of the endogenous protein (Figure S5A).

Using these cell lines, we depleted endogenous RNF168 by RNAi prior to tet-mediated induction. The cells were then irradiated and processed for 53BP1 immunofluorescence. Utilizing this approach, we found that the RNF168 RING finger was critical to promote the formation of 53BP1 foci (Figures 3 and S10). Interestingly, the A179G point mutation in MIU1 did not impair RNF168 function, whereas the MIU2 A450G and double A179G/A450G mutation(s) progressively led to a large reduction in the number of 53BP1 foci-positive cells following irradiation (Figure 3). Examination of the 53BP1 focus morphology revealed that the 53BP1 foci formed in the A179G/A450G line were markedly smaller than those of wild-type cells (Figure 3B). A similar picture emerges when 53BP1 focus formation was examined in cells expressing RNF168 lacking one or both MIU motifs. We found that deletion of MIU1 had little effect on the ability of cells to form 53BP1 IR-induced foci, whereas deletion of MIU2 impaired 53BP1 focus formation to levels similar to those observed with the A179G/A450G double mutation (Figure 3). However, in the context of the MIU2 deletion, MIU1 nevertheless played some function, as deletion of both MIUs further impaired 53BP1 relocalization to DSB sites to background levels (Figure 3). Therefore, we concluded that RNF168 requires its RING finger and MIU motifs (primarily MIU2) to promote DNA damage signaling.

Figure 1. RNF168 Promotes the Accumulation of 53BP1 and BRCA1 IR-Induced Foci

(A) HeLa cells seeded in 384-well plates were transfected with the indicated esiRNA. At 24 hr posttransfection, cells were irradiated with a 10 Gy dose, fixed 1 hr post-IR, and processed for 53BP1 immunofluorescence and quantitation as described previously (Kolas et al., 2007). The 53BP1 focus index represents the number of 53BP1 foci detected in a confocal slice using our spot-finding algorithm. Data are represented as the mean ± SEM (n = 4).

(B) HeLa cells were transfected first with either nontargeting (siCTRL) or RNF168 (siRNF168) siRNAs. After transfection, cells were reseeded and transfected with an empty control vector (empty) or a siRNA-resistant FLAG-tagged RNF168 expression vector (RNF168*). Twenty-four hours later, cells were irradiated with a 10 Gy dose, fixed 1 hr post-IR, and processed for 53BP1 immunofluorescence. The upper panels display representative micrographs, and the data in the lower panel represent the mean ± SEM (n = 3).

(C) Representative knockdown of RNF168 in HeLa cells using esiRNA. LUC, luciferase.

(D) U2OS cells transfected either with control (siCTRL) or RNF168 (siRNF168) siRNAs were either mock treated (−IR) or irradiated with a 10 Gy dose (+IR). At 1 hr post-IR, cells were fixed and processed for immunofluorescence using the indicated antibodies. Quantitation of the data can be found in Figure S2.

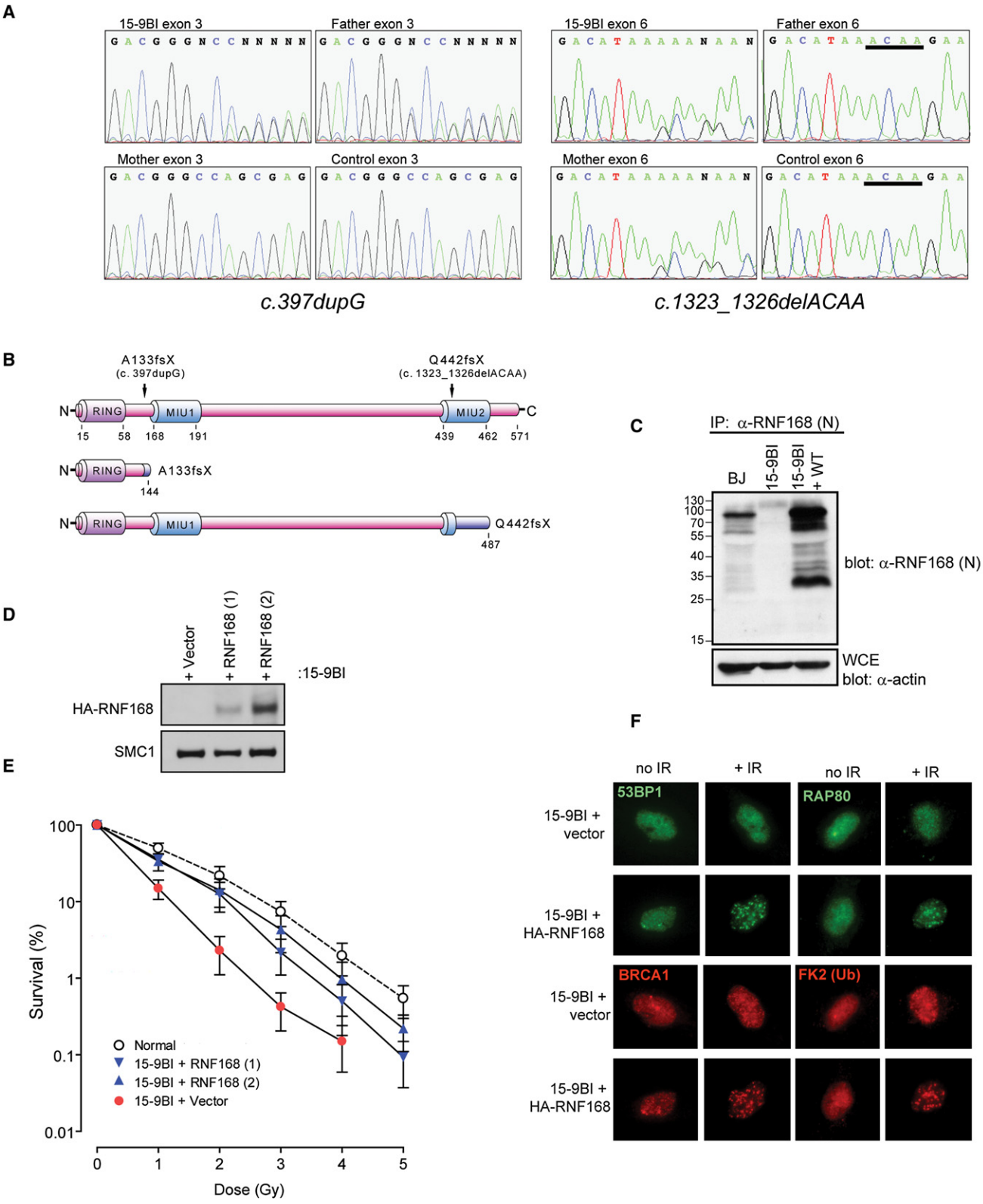

Figure 2. *RNF168* Is the Gene Mutated in the RIDDLE Syndrome

(A) Sequencing of the *RNF168/RNF168* exons in cells derived from the 15-9BI RIDDLE patient and his parents.

RNF168 Accumulates at Sites of DNA Damage in an MIU-Dependent Manner

The functional importance of RNF168 for the DNA damage response prompted us to test whether RNF168 itself accumulated at sites of DNA damage. We found that endogenous RNF168 rapidly relocalized to γ-H2AX-positive subnuclear foci, as soon as 5 min after irradiation (Figure 4A). The loss of these foci in cells transfected with RNF168 siRNA confirmed the specificity of the antibody in immunofluorescence (Figure S6A). The rapid accumulation of RNF168 into foci was also observed in cells expressing green fluorescent protein (GFP)-tagged versions of RNF168 (Figure S6B). Collectively, these observations suggest that RNF168 acts locally at the site of DNA breaks to promote the DNA damage response.

Next, we mapped the domains of RNF168 required for its localization to sites of DNA damage. We introduced, in the context of GFP-RNF168, mutations that disrupted the RING finger or MIU motifs as well as the RIDDLE syndrome mutations described above. Wild-type RNF168 and the allelic series presented were transiently (Figures 4B and S5B) or stably (Figure S7) transfected into HeLa and U2OS cells, respectively, for foci analyses. Surprisingly, we found that deletion of the RING finger (ΔRING) did not affect RNF168 focus formation after IR (Figures 4B and 4C). In contrast, RNF168 accumulation at sites of DNA damage required functional MIU motifs. Whereas the A179G and A450G mutations individually had a minimal impact on the ability of RNF168 to form foci, we found that the A450G mutation in MIU2 impaired the maintenance of RNF168 at sites of DNA damage (see the 4 hr and 8 hr time points, Figure S7). The double A179G/A450G mutation severely impaired, but did not totally abolish, the ability of RNF168 to form foci especially at early time points after IR (Figures 4B, 4C, and S7). This latter result was consistent with the observation that the A → G point mutants are not entirely null for ubiquitin binding. We next examined the impact of MIU deletions on RNF168 localization. Deletion of MIU1 (ΔMIU1) did not impair RNF168 accumulation at sites of DNA damage (Figures 4B and 4C). In contrast, deletion of the MIU2 domain (alone or in the context of the ΔMIU1/2 mutant) severely impaired the focal redistribution of RNF168 (Figures 4B and 4C). These results indicate that RNF168 localization at sites of DNA damage depends on its MIU motifs, primarily mediated through MIU2.

Finally, we examined whether the A133fsX and Q442fsX mutant RNF168 proteins could relocalize to DSBs. As shown in Figure 4B, the product of neither RIDDLE allele was able to form IR-induced foci, in line with the observation that they both lack the MIU2 motif.

H2A Ubiquitylation Mediates Accumulation of RNF168 at DNA Lesions

As a means to place RNF168 in the DNA damage signaling cascade, we quantitated RNF168 foci in cells depleted of MDC1, RNF8, NBS1, 53BP1, and BRCA1. As shown in Figure 5AB, RNF168 foci are abrogated in cells depleted of MDC1 and RNF8, whereas they are unaffected in cells depleted of NBS1, 53BP1, and BRCA1. These observations indicate that RNF168 acts either downstream or at the same level as RNF8 to promote DNA damage signaling. To distinguish between these two possibilities, we examined RNF8-YFP focus formation in RNF168-depleted cells. Strikingly, upon RNF168 depletion, RNF8 still accumulated at DSBs (Figure 5C), strongly indicating that RNF168 acts downstream of RNF8.

This latter result, coupled with the critical importance of the MIUs for formation of RNF168 foci, suggested that RNF168 is recruited to DNA lesions by binding to ubiquitylated substrates of RNF8. In support of this possibility, we found that the RNF8 RING finger was necessary to promote RNF168 foci (Figures 5D and 5E and S5B). In addition, we ascertained that UBC13, proposed to be the RNF8 E2, was also critical for RNF168 focus formation (Figure 5F). Lastly, we took advantage of the observation that MG132 treatment greatly reduces H2A ubiquitylation (Mailand et al., 2007). As a consequence, MG132 inhibits the formation of BRCA1 and 53BP1 IR-induced foci while having little or no effect on RNF8 focus formation (Jacquemont and Taniguchi, 2007; Mailand et al., 2007). Addition of MG132 to cells prior to irradiation profoundly inhibited the accumulation of RNF168 at sites of DNA damage (Figure S6C). Together, these results demonstrate that RNF168 localization at sites of DNA damage depends on protein ubiquitylation carried out by RNF8-UBC13.

Because histones H2A and H2AX have been shown to be targets of the RNF8-UBC13 E3 ligase activity (Huen et al., 2007; Mailand et al., 2007), we therefore examined whether RNF168, via its MIUs, can physically interact with ubiquitylated H2A (uH2A). We transfected FLAG-RNF168 (wild-type or MIU deletion mutants) into HEK293 T cells and prepared chromatin-enriched fractions that were subjected to FLAG immunoprecipitation. As shown in Figure 6A, wild-type RNF168 interacts with uH2A, in particular the diubiquitylated form. This interaction is slightly reduced in the ΔMIU1 mutant but is abolished by the ΔMIU2 or ΔMIU1/2 mutations. Remarkably, the requirement for the MIU2 motif for the RNF168-uH2A interaction mirrors the requirement for formation of RNF168 IR-induced foci. Next, we examined whether this interaction was dependent on DNA damage and RNF8. As expected, we observed that the RNF168-uH2A interaction is stimulated by DNA damage and is greatly

(B) Schematic structure of RNF168. The predicted mutant proteins encoded by the maternal (*c.1323_1326 delACAA*) and paternal (*c.397 dupG*) *RNF168* mutant alleles are shown. The blue shaded area of the RIDDLE-associated mutant proteins marks sequences produced by the frameshifted open reading frame.

(C) Whole-cell extracts (WCE) from BJ cells, 15-9BI cells transduced with either an empty retrovirus (15-9BI) or wild-type RNF168 (15-9BI + WT), were subjected to immunoprecipitation followed by immunoblotting with the RNF168 (N) antibody. Actin is used as loading control for the WCE.

(D) WCE from 15-9BI cells transduced with a retrovirus containing no insert (+vector) or HA-RNF168 (+RNF168; two independent clones are presented) were separated on SDS-PAGE and subjected to HA and SMC1 immunoblotting. SMC1 is used as loading control.

(E) Clonogenic survival of the 15-9BI cells described in (D) following irradiation. Data are represented as mean ± SEM (n = 3).

(F) Control-transfected (15-9BI+vector) or RNF168-complemented (15-9BI + RNF168) RIDDLE cells were either mock treated (no IR) or irradiated with a dose of 5 Gy. Cells were fixed 1 hr post-IR and processed for 53BP1, RAP80, BRCA1, and anti-ubiquitin conjugate (FK2) immunofluorescence. Representative micrographs are shown. A time course of this experiment is shown in Figure S4.

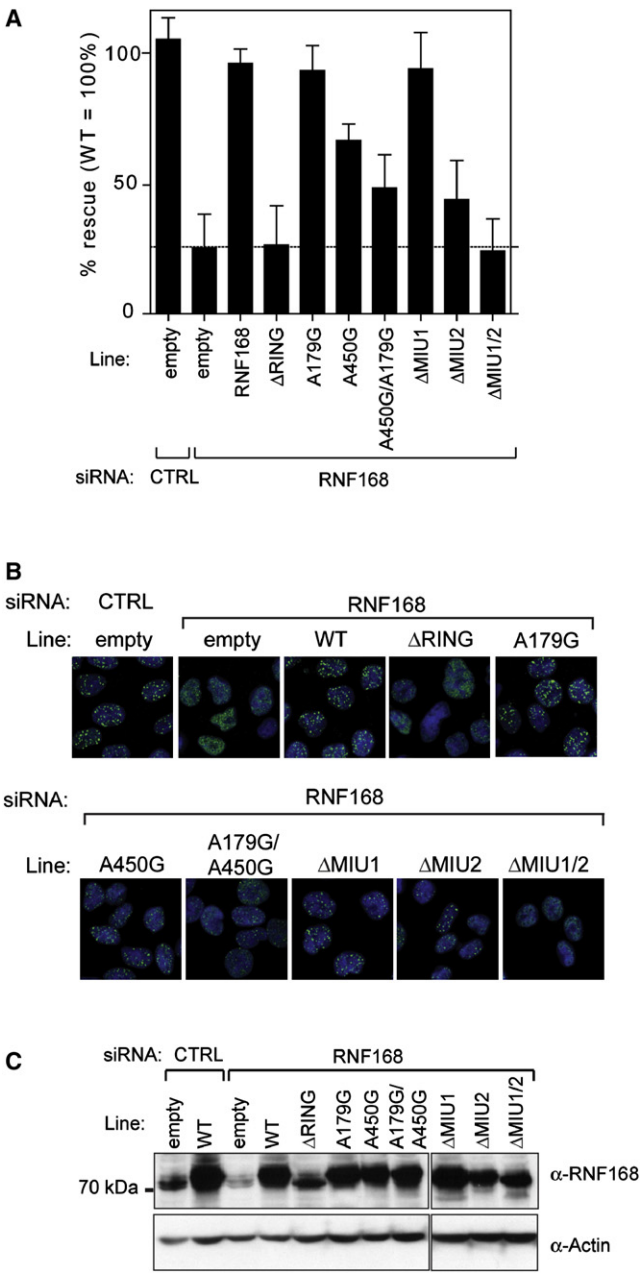

Figure 3. RNF168 Function Requires Its RING and MIU Motifs

(A–C) Flp-In/T-Rex HCT116 cell lines expressing the indicated RNF168 mutants under a tetracycline-inducible promoter were seeded into 10 cm dishes and transfected with nontargeting (CTRL) or RNF168 siRNA. Cells were then reseeded onto coverslips (for immunofluorescence) and in 6 cm dishes to analyze protein expression. RNF168 expression was induced for 24 hr as described in the Experimental Procedures. Cells were then irradiated (10 Gy) and fixed 1 hr post-IR to be processed for immunofluorescence (B), quantitation of 53BP1 foci (A), and immunoblotting (C). Data in (A) are represented as the mean ± SEM (n = 4).

reduced in cells treated with RNF8 siRNA (Figures 6B and 6C). These results suggest that RNF8-dependent H2A ubiquitylation mediates the accumulation of RNF168 at sites of DNA damage.

RNF168 Is a UBC13-Dependent E3 Ubiquitin Ligase

The functional importance of the RNF168 RING finger prompted us to examine whether RNF168 is a bona fide E3 ubiquitin ligase. We expressed full-length RNF168, as well as the C19S and ΔRING mutants, as recombinant GST fusion proteins in bacteria (Figure S9A). We then assembled in vitro ubiquitylation reactions in which the RNF168 proteins were added to a panel of E2 enzymes (UBC1, UBC3, UBC7, and UBC13/MMS2) in addition to the E1 (UBE1), ATP, and ubiquitin. Protein ubiquitylation was assessed by immunoblotting using the FK2 antibody to detect conjugated ubiquitin. As shown in Figure 6D, RNF168 robustly autoubiquitylates when reactions are carried out in the presence of the UBC13-MMS2 complex, but not with any other E2 enzyme tested. Furthermore, this autoubiquitylation activity of RNF168 requires a functional RING finger since the C19S mutation or deletion of the RING finger completely abolished ubiquitin conjugation (Figure 6D). Identical results were obtained when RNF168 immunopurified from HEK293 T cells was used in similar ubiquitylation assays (Figure S9B). We also examined whether the E3 activity of RNF168 was affected by the MIU point mutations or the RIDDLE syndrome mutations. Predictably, these mutants displayed normal levels of E3 ligase activity since they do not impact the RING finger (Figure S9C).

The notion that UBC13 acts as the RNF168 E2 is significant given the importance of UBC13 in orchestrating the response to IR. To further explore this relationship, we tested whether UBC13 and RNF168 interact together using coimmunoprecipitation studies. We detected an interaction of either endogenous (Figure 6E) or epitope-tagged RNF168 (Figure S9D) with UBC13 that was dependent on its RING finger domain. RNF168 is, therefore, an E3 ubiquitin ligase that utilizes UBC13 as its E2.

Next, we sought to determine what type of ubiquitylation linkage is catalyzed by RNF168-UBC13. Initially, we carried out in vitro ubiquitylation assays in which different ubiquitin lysine mutants were used. We found that RNF168 generates ubiquitin conjugates with wild-type, K6R, and K48R ubiquitin, but not with the K63R ubiquitin mutant or a ubiquitin version that lacks all lysine residues (K0) (Figure 6F). These results indicate that RNF168, in the presence of UBC13, catalyzes K63-linked polyubiquitin (UbK63) chains, a result confirmed when the products of the above reactions were probed with an anti-UbK63 antibody (Figure 6F).

To determine whether RNF168 is also necessary for the formation of K63-linked ubiquitin conjugates in vivo, we took advantage of novel human monoclonal antibodies directed against K48 (UbK48) or UbK63 chains (Newton et al., 2008). These antibodies were used in immunofluorescence experiments to determine what type of ubiquitin conjugation occurred at sites of DNA damage. As shown in Figures 6G and S10, UbK63 (but not UbK48; data not shown) were detected in IR-induced foci that colocalize with γ-H2AX. Not surprisingly, the formation of UbK63 chains was entirely dependent on UBC13, the only E2 known to catalyze such chain linkage (Figure 6G). Importantly, depletion of RNF8 or RNF168 strongly impaired formation of UbK63 foci, consistent with these enzymes acting with UBC13 at sites of DNA damage. Moreover, deletion of the RNF168 RING finger abolished the formation of UbK63 foci (Figure S10), indicating that the E3 ligase activity of RNF168 is necessary to

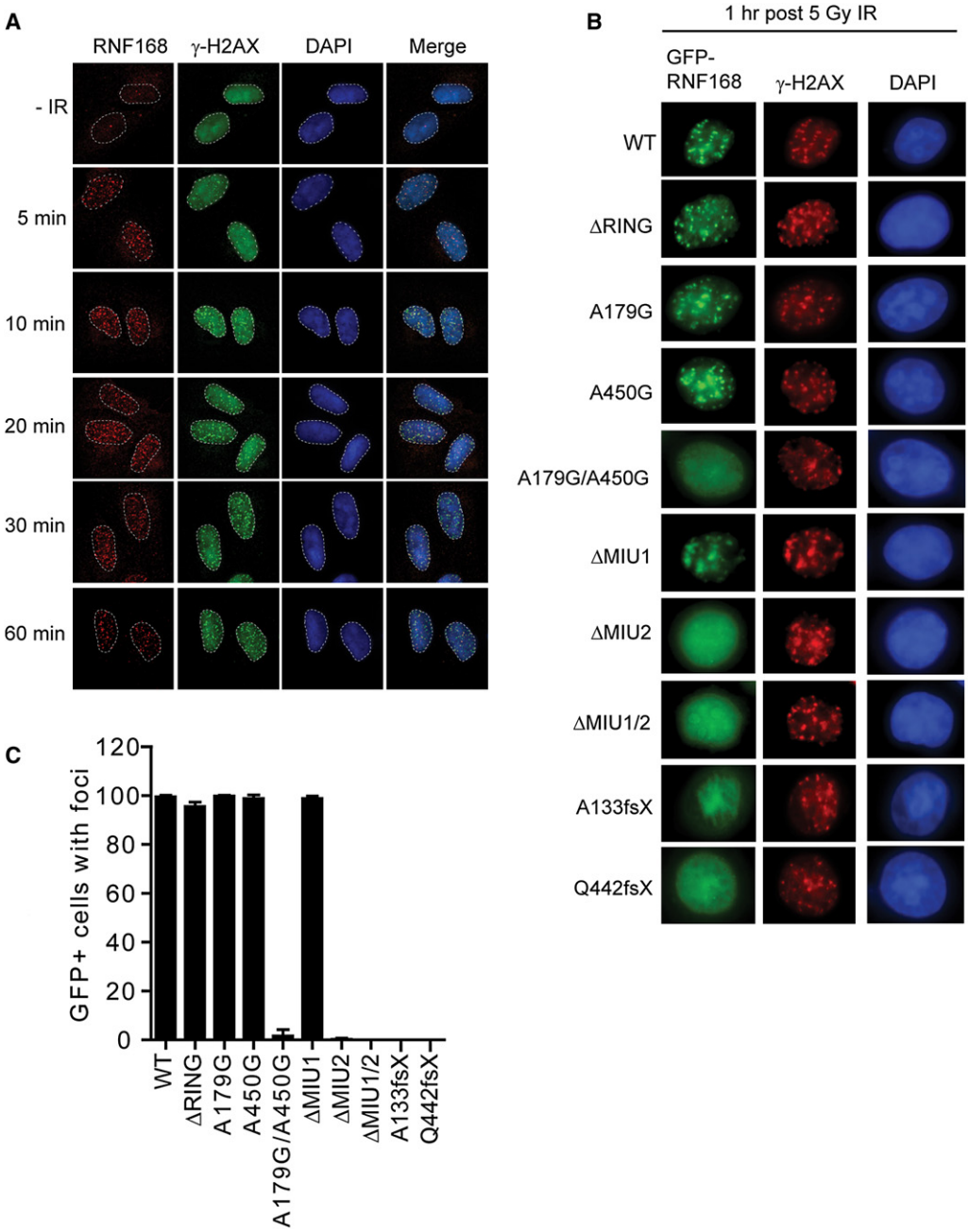

Figure 4. RNF168 Accumulates at Sites of DNA Damage

(A) U2OS cells were either irradiated with a 10 Gy dose or mock treated (−IR). After the indicated time points, cells were fixed and processed for RNF168 and γ-H2AX immunofluorescence. DNA was stained with DAPI.

(B) HeLa cells transfected with the indicated GFP-RNF168 expression vectors were irradiated with a 5 Gy IR dose. At the indicated time points, cells were fixed and processed for GFP fluorescence and γ-H2AX immunofluorescence. DNA was stained with DAPI.

(C) Quantitation of (B). Data are represented as the mean ± SD (n = 3).

build UbK63 at DNA damage sites. Lastly, depletion of 53BP1 and especially BRCA1, another E3 ligase, did not impair the formation of K63-linked ubiquitin conjugates at DSBs (Figure 6G). These results indicate that RNF168 catalyzes K63-linked ubiquitylation on the chromatin that surrounds DNA lesions.

RNF168 Targets H2A-Type Histones

Ubiquitylated H2A can be detected in IR-induced foci that colocalize with γ-H2AX (Nicassio et al., 2007). Therefore, we examined whether formation of uH2A foci was dependent on RNF8, RNF168, or UBC13. To our surprise, we found that the formation

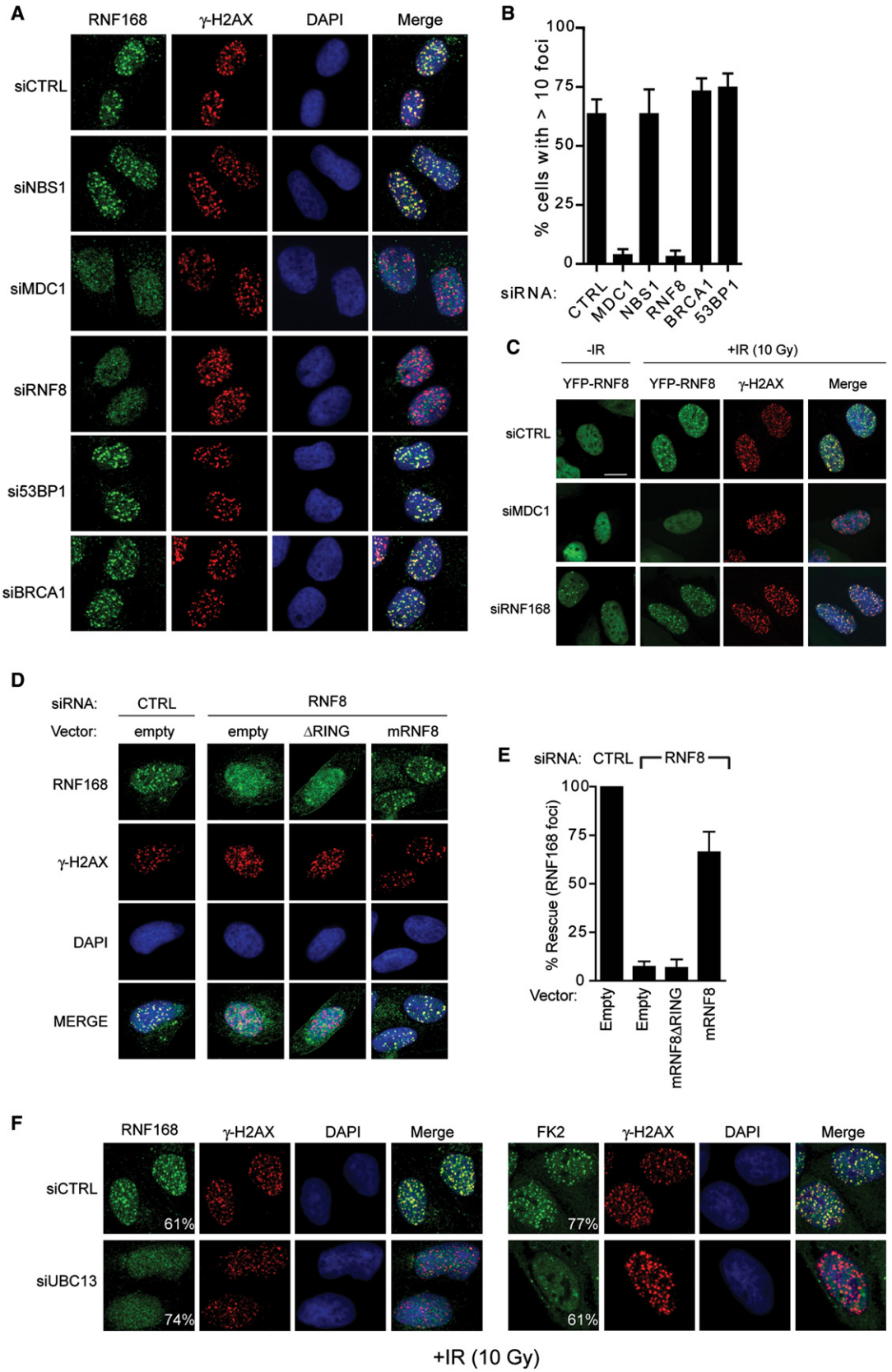
A
RNF168
γ-H2AX
DAPI
Merge
siCTRL
siNBS1
siMDC1
siRNF8
si53BP1
siBRCA1
B
% cells with > 10 foci
100
75
50
25
0
siRNA:
CTRL
MDC1
NBS1
RNF8
BRCA1
53BP1
C
-IR
+IR (10 Gy)
YFP-RNF8
YFP-RNF8
γ-H2AX
Merge
siCTRL
siMDC1
siRNF168
D
siRNA:
CTRL
RNF8
Vector:
empty
empty
ΔRING
mRNF8
RNF168
γ-H2AX
DAPI
MERGE
E
siRNA: CTRL
RNF8
% Rescue (RNF168 foci)
100
75
50
25
0
Vector:
Empty
Empty
mRNF8ΔRING
mRNF8
F
RNF168
γ-H2AX
DAPI
Merge
FK2
γ-H2AX
DAPI
Merge
siCTRL
61%
77%
siUBC13
74%
61%
+IR (10 Gy)

of uH2A foci was not only dependent on RNF8-UBC13, but was also dependent on the presence of RNF168 (Figure 7A). Formation of uH2A foci was independent of BRCA1 and 53BP1, pointing to RNF168 as being critical for the generation of uH2A IR-induced foci. Importantly, cells expressing the RNF168 ΔRING were unable to support uH2A foci formation, arguing against the possibility that the physical binding of RNF168 to uH2A decreased its removal from chromatin (Figure S10). H2A-type histones might, therefore, be targeted in vivo by both RNF8 and RNF168.

The above results suggest that RNF168 and RNF8 have overlapping sets of substrates. However, another possibility might be that RNF168 is necessary for RNF8 action at sites of DNA damage. To distinguish between these possibilities, we examined whether RNF168 overexpression in RNF8-depleted cells restored 53BP1 focus formation. As shown in Figures 7B and S5D, overexpression of wild-type RNF168 indeed restored 53BP1 focus formation in more than 50% of the RNF8-depleted cells. Together, these results support a model whereby RNF168 and RNF8 have overlapping substrates and RNF168 lies downstream of RNF8.

Next, we directly tested whether RNF168 can ubiquitylate H2A in E3 ligase reactions in which either recombinant H2A or H2B was added to RNF168-UBC13. We observed that H2A, not H2B, is specifically ubiquitylated by RNF168 (Figure 7C), strongly supporting the possibility that H2A-type histones are RNF168 substrates.

Finally, to gain direct evidence that RNF168 catalyzes the formation of ubiquitylated H2A, we examined the ubiquitylation status of H2A in response to DNA damage (Huen et al., 2007). We isolated bulk histones by acid extraction of irradiated HeLa cells transfected with control or RNF168 siRNAs. As shown in Figure 7D, we observed that RNF168 depletion reduces the levels of radiation-induced histone H2A ubiquitylation, in particular the diubiquitylated form. We conclude that RNF168 can catalyze the ubiquitylation of H2A-type histones in response to DNA damage.

DISCUSSION

We report that mutations in *RNF168* are responsible for RIDDLE syndrome. RNF168 depletion impairs the accumulation of 53BP1 and BRCA1 at sites of DNA lesions and impacts both the S and G2/M checkpoints (K.T., S.P., D.D., and G.S.S., unpublished data). Although it is unclear which aspects of RNF168 deficiency contribute to the syndrome phenotype, we speculate that, given the known function of 53BP1 in promoting DSB repair during CSR, it is the failure of 53BP1 to be relocalized during this process that is the underlying cause of the immunodeficiency in this patient. Although we previously failed to detect any gross defects in NHEJ in RIDDLE cells (Stewart et al., 2007), the recent demonstration of a role for 53BP1 in promoting nonclassical NHEJ during V(D)J recombination (Difilippantonio et al., 2008) suggests that RNF168 may act to organize the chromatin to facilitate long-range NHEJ.

The Action of RNF8 and RNF168 at Sites of DNA Damage

RNF8, RNF168, and BRCA1 define an emerging regulatory ubiquitylation cascade initiated by DSBs. Our observation that RNF8 and RNF168 are sequentially recruited to DNA lesions strongly suggests that they act successively, possibly by ubiquitylating separate substrates (Figure 7E). However, we also report evidence that RNF168 amplifies RNF8-dependent H2A ubiquitylation. With respect to H2A ubiquitylation, RNF8 acts primarily to increase the local concentration of RNF168 at sites of DNA damage by initiating the ubiquitylation of H2A-type histones, which then act as a signal to physically recruit RNF168 via its MIU motifs to the sites of DNA damage (Figure 7E). In support of this model, in an accompanying paper, Doil et al. also describe the identification of RNF168 and propose a similar model of RNF168 action at sites of DNA damage (Doil et al., 2009 [this issue of *Cell*]). The cooperation of RNF8 and RNF168 to ubiquitylate histones as a means to reorganize chromatin is not a unique phenomenon because H2A and H2B ubiquitylation during transcriptional regulation also requires the action of two E3 ligases, Ring1a and Ring1b (for H2A) and RNF20 and RNF40 (for H2B) (Wang et al., 2004; Zhu et al., 2005).

The availability of novel antibodies against K63-linked ubiquitin chains (Newton et al., 2008) has allowed us to demonstrate that RNF168 promotes the formation of K63-linked ubiquitin conjugates at sites of DNA damage. However, at this stage, we have been unable to provide in vivo evidence that UbK63 chains are assembled on H2A or H2AX. Given that K63-linked ubiquitylation clearly plays an important role during the organization of the DNA damage response (Sobhian et al., 2007), the identification of additional targets of RNF8 and RNF168,

Figure 5. RNF168 Acts Downstream of RNF8

(A) U2OS cells transfected either with control (siCTRL) or the indicated siRNAs were irradiated with a 10 Gy dose. At 1 hr after irradiation, cells were fixed and processed for RNF168 and γ-H2AX immunofluorescence. Controls for the effectiveness of the siRNAs used in this experiment can be found in Figure S8.

(B) Quantitation of RNF168 foci from the experiment described in (A). Data are represented as the mean ± SD (n = 3).

(C) U2OS cells stably transfected with YFP-RNF8 were transfected either with control (siCTRL), MDC1 (siMDC1), or RNF168 (siRNF168) siRNAs. At 36 hr post-transfection, cells were either mock treated (−IR) or X irradiated with a 10 Gy dose (+IR). At 1 hr after irradiation, cells were fixed and processed for YFP and γ-H2AX immunofluorescence. DNA was stained with DAPI. Scale bar, 16 μm.

(D) HeLa cells were transfected first with either nontargeting control (CTRL) or RNF8 (RNF8) siRNAs. After transfection, cells were reseeded onto coverslips and transfected either with an empty control vector (empty) or murine FLAG-RNF8 vectors (mRNF8 or mRNF8 ΔRING). Murine RNF8 mRNA is resistant to a human siRNA pool against RNF8 (Kolas et al., 2007). At 24 hr after plasmid transfections, cells were irradiated with a 10 Gy dose, fixed 1 hr post-IR, and processed for RNF168 immunofluorescence. Refer to Figure S5C for control immunoblots.

(E) Quantitation of RNF168 foci from the experiment described in (D). Data are represented as the mean ± SD (n = 3).

(F) U2OS cells transfected either with control (siCTRL) or UBC13 siRNAs were irradiated with a 10 Gy dose. At 4 hr after irradiation, cells were fixed and processed for RNF168, γ-H2AX, and conjugated ubiquitin (FK2) immunofluorescence. The percentage of cells in the population that display the represented phenotype is indicated on the micrograph.

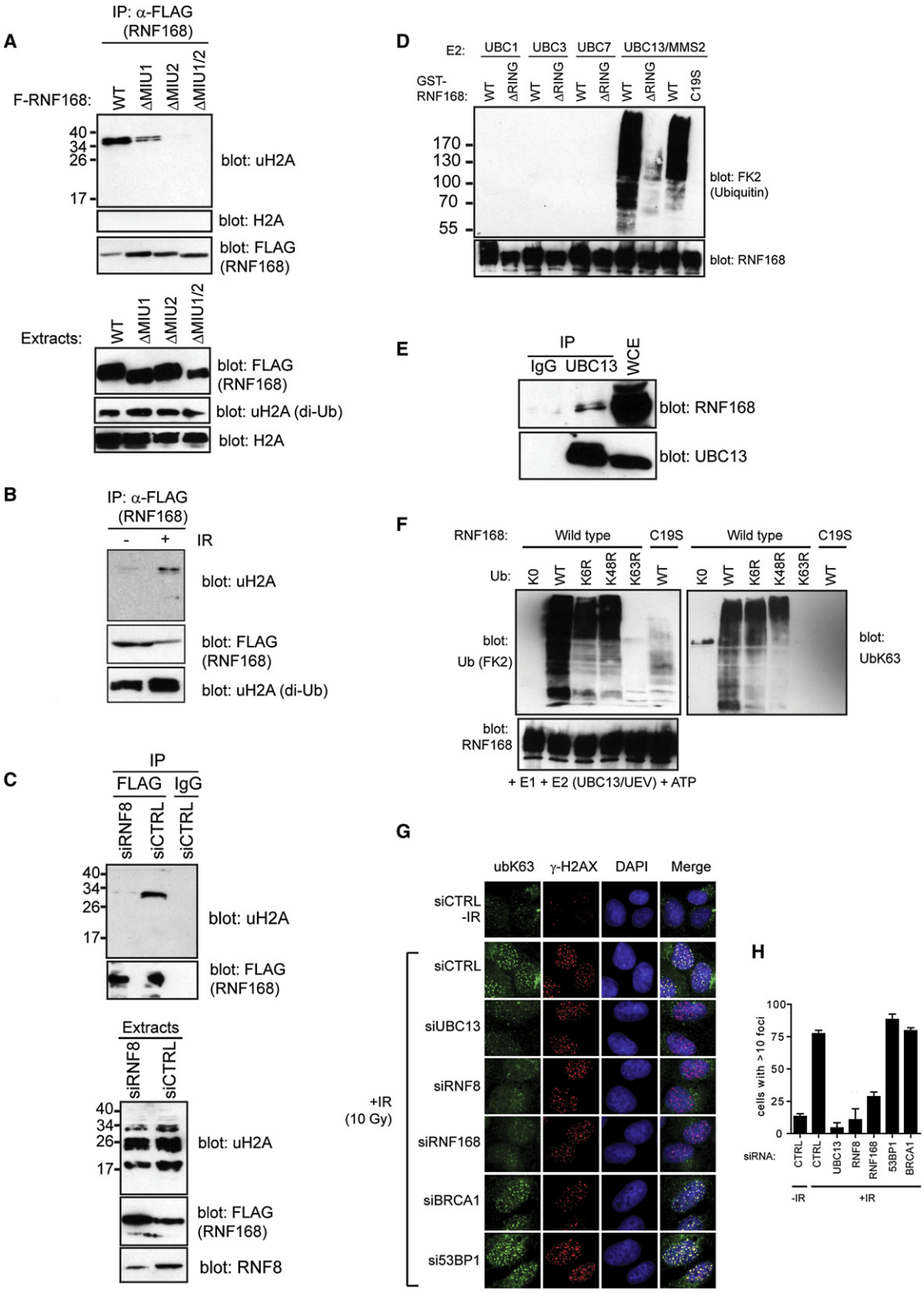
A
IP: α-FLAG (RNF168)
F-RNF168: WT ΔMIU1 ΔMIU2 ΔMIU1/2
40
34
26
17
blot: uH2A
blot: H2A
blot: FLAG (RNF168)
Extracts: WT ΔMIU1 ΔMIU2 ΔMIU1/2
blot: FLAG (RNF168)
blot: uH2A (di-Ub)
blot: H2A
B
IP: α-FLAG (RNF168)
- + IR
blot: uH2A
blot: FLAG (RNF168)
blot: uH2A (di-Ub)
C
IP
FLAG IgG
siRNF8 siCTRL siCTRL
40
34
26
17
blot: uH2A
blot: FLAG (RNF168)
Extracts
siRNF8 siCTRL
40
34
26
17
blot: uH2A
blot: FLAG (RNF168)
blot: RNF8
D
E2: UBC1 UBC3 UBC7 UBC13/MMS2
GST-RNF168: WT ΔRING WT ΔRING WT ΔRING WT ΔRING WT C19S
170
130
100
70
55
blot: FK2 (Ubiquitin)
blot: RNF168
E
IP
IgG UBC13 WCE
blot: RNF168
blot: UBC13
F
RNF168: Wild type C19S Wild type C19S
Ub: K0 WT K6R K48R K63R WT K0 WT K6R K48R K63R WT
blot: Ub (FK2)
blot: UbK63
blot: RNF168
+ E1 + E2 (UBC13/UEV) + ATP
G
ubK63 γ-H2AX DAPI Merge
siCTRL -IR
+IR (10 Gy)
siCTRL
siUBC13
siRNF8
siRNF168
siBRCA1
si53BP1
H
cells with >10 foci
100
75
50
25
0
siRNA: CTRL CTRL UBC13 RNF8 RNF168 53BP1 BRCA1
-IR
+IR

especially those modified with UbK63, will be needed to resolve how this novel protein ubiquitylation pathway promotes DNA repair, checkpoint signaling, and the developmental processes associated with the DNA damage response.

Finally, we expect that the discovery of *RNF168* will lead to the identification of additional RIDDLE patients and that those will, in turn, result in a better definition of the clinical phenotype of RIDDLE syndrome. It is still unclear whether RIDDLE syndrome is associated with genome instability or increased tumor incidence. Given that RNF168 promotes the accumulation of BRCA1 to sites of DNA damage and is likely to function in CSR-associated DNA repair, a process tightly linked with the development of lymphoid malignancies, it is conceivable that *RNF168* might act as a tumor suppressor gene and play a role in the development of sporadic malignancies, particularly those of lymphoid origin. In this respect, it might be of significance that the father of the RIDDLE patient has developed B cell chronic lymphocytic leukemia. Therefore, one of the important future challenges will be to determine whether *RNF168* acts as a tumor suppressor gene.

EXPERIMENTAL PROCEDURES

Cell Culture and Plasmid Transfection

U-2-OS (U2OS) cells were cultured in McCoy's medium, and HeLa and HEK293 T cells were cultured in DMEM. The 15-9BI cells were cultured as described in Stewart et al. (2007). Stable and transient transfections were performed using Effectene (QIAGEN) or Lipofectamine 2000 (Invitrogen), respectively, following the manufacturer's protocol.

Quantitation of 53BP1 Foci by High-Content Microscopy

Cell imaging using the Opera system (PerkinElmer) and image segmentation using Acapella software (PerkinElmer) were performed exactly as described in Kolas et al. (2007).

RNA Interference

All siRNAs employed in this study were SMARTpools (ThermoFisher) or individual siRNAs deconvolved from the SMARTpool. esiRNAs were produced exactly as described in Kittler et al. (2005). All RNAi transfections were performed using Dharmafect 1 (ThermoFisher) or Oligofectamine (Invitrogen).

Generation of a siRNA-Resistant Flag-RNF168-Expressing Vector

To generate RNF168 constructs resistant to RNF168 siRNA#4 from Dharmacon (D-007152-04), we introduced the following underlined silent mutations in RNF168: 5′-GAGGAGTCGTGTTTATTGA-3′.

Antibodies

We employed the following antibodies: 53BP1 (clone 19, BD Biosciences; NB100-305, Novus Biologicals), MDC1 (clone MDC1-50, Sigma-Aldrich; AbD, Serotec), γ-H2AX (clone JBW301, Upstate), BRCA1 (clones MS110, Calbiochem; D9, Santa Cruz), RAP80 (Bethyl Laboratories), histone H3 phosphoserine 10 (clone 6G3, Cell Signaling Technologies), conjugated ubiquitin (clone FK2, Stressgen), UbK63 (clone Apu3.A8, Genentech), UbK48 (clone Apu2.07, Genentech), UbK63 (clone HWA4C4, Biomol International), RNF8 (gift of J. Chen), uH2A (clone E6C5, Upstate), uH2B (clone NRO3, Médimabs), GST (clone B4, Santa Cruz), Nbs1 (Novus Biologicals), RIF1 (Bethyl Laboratories), FLAG (M2, Sigma), actin (clone JLA20, Calbiochem), HA (clone 12CA5), and UBC13 (clone 4E11, Zymed). The RNF168 polyclonal antibodies were raised against GST-RNF168$^{1–200}$ (antibody N) and GST-RNF168$^{380–571}$ (antibody C) fusion proteins and were affinity purified.

E3 Ubiquitin Ligase Assays

Ubiquitin ligase assays were performed as follows. Assays were set up in a total volume of 25 μl in 50 mM Tris-HCl (pH 8.0) and 1 mM DTT. Recombinant GST-RNF168 (0.2 μM) was added to 0.4 μM of the indicated E2 enzymes (Boston Biochem), 0.0125 μM E1 and 16 μM ubiquitin (Boston Biochem). Reactions were initiated by the addition of ATP (2 mM) and $MgCl_2$ (5 mM).

SUPPLEMENTAL DATA

The Supplemental Data include Supplemental Experimental Procedures, ten figures, and one table and can be found with this article online at http://www.cell.com/supplemental/S0092-8674(09)00005-1.

ACKNOWLEDGMENTS

We are grateful to C. Handy, A. Datti, and T. Sun for their invaluable help with the siRNA screen and to AC Gingras, T. Thomson, F. Sicheri, B. Wouters, J. Chen, S. Jackson, Genentech, and J. Lukas for important reagents. We are also grateful to Jiri and Claudia Lukas for sharing results prior to their publication. G.S.S., K.T., and E.S.M. are funded by a CR-UK career development fellowship (ref: C17183/A5592). A.M.R.T. and P.J.B. are supported by a CR-UK program grant. T.S. is funded by a Leukemia Research Fund-UK program grant. S.P. holds a Boehringer Ingelheim Foundation studentship; A.K.A.-H. holds a postdoctoral fellowship from the TD Bank; N.K.K. is a Terry Fox

Figure 6. RNF168 Binds to uH2A and Is a UBC13-Dependent E3 Ligase

(A) HEK293 T cells transfected with the indicated FLAG-RNF168 vectors were irradiated (20 Gy), and chromatin-enriched extracts (CEE) were prepared 4 hr post-IR. (Upper panel) CEE were subjected to FLAG immunoprecipitation and then separated on SDS-PAGE and subjected to FLAG, ubiquitylated (uH2A), or total H2A (H2A) immunoblotting. (Lower panel) CEE were probed with the same antibodies as above. The diubiquitylated H2A band is shown for the uH2A blot.

(B) HEK293 T transfected with FLAG-RNF168 were irradiated with a 20 Gy dose (+IR) or left untreated (−IR). At 4 hr postirradiation, CEE were prepared and subjected to FLAG immunoprecipitation. Precipitates were separated on SDS-PAGE and subjected to FLAG and ubiquitylated (uH2A) immunoblotting.

(C) HEK293 T cells were first transfected with nontargeting control (siCTRL) or RNF8 (siRNF8) siRNAs. Cells were then transfected with the indicated FLAG-RNF168 expression constructs and irradiated (20 Gy), and CEE were prepared 4 hr post-IR. (Upper panel) The extracts were subjected to FLAG immunoprecipitation, separated on SDS-PAGE, and immunoblotted with antibodies to FLAG, uH2A, or H2A. (Lower panel) CEE were probed with the indicated antibodies.

(D) In vitro ubiquitylation assays employing recombinant GST-RNF168 proteins were assembled as described in the Experimental Procedures. The reaction products were analyzed by immunoblotting with anti-ubiquitin conjugate (FK2) and anti-RNF168 antibodies.

(E) HEK293 T WCE were subjected to UBC13 immunoprecipitation (IP). The immunoprecipitates were separated on SDS-PAGE and subjected to UBC13 and RNF168 immunoblotting.

(F) In vitro ubiquitylation assays using recombinant GST-RNF168 proteins were assembled in the presence of wild-type or the indicated mutated ubiquitin proteins. The reaction was analyzed by immunoblotting with ubiquitin conjugate (FK2) (upper-left panel), RNF168 (lower-left panel), and UbK63 antibodies (right panel).

(G) U2OS cells transfected either with control (siCTRL) or the indicated siRNAs were irradiated with a 10 Gy dose. At 4 hr after irradiation, cells were fixed and processed for K63-linked ubiquitin chain (UbK63) and γ-H2AX immunofluorescence. Controls for the effectiveness of the siRNAs can be found in Figure S8. DNA was counterstained with DAPI.

(H) Quantitation of UbK63 foci from the experiment described in (G). Foci-positive cells were defined as cells with more than ten defined UbK63 foci. Data are represented as the mean ± SD (n = 3).

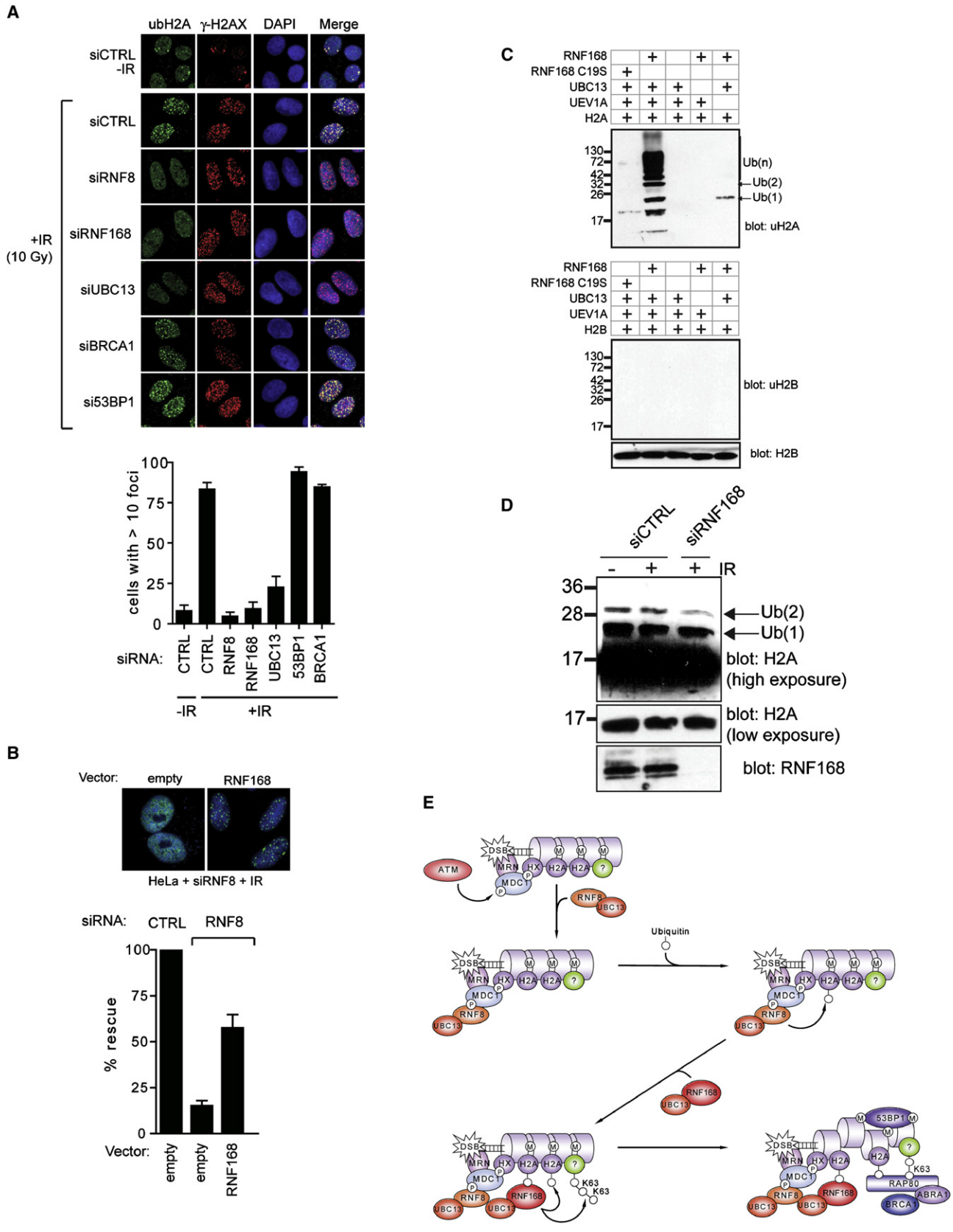
A
ubH2A
γ-H2AX
DAPI
Merge
siCTRL -IR
+IR (10 Gy)
siCTRL
siRNF8
siRNF168
siUBC13
siBRCA1
si53BP1
cells with > 10 foci
siRNA:
CTRL
CTRL
RNF8
RNF168
UBC13
53BP1
BRCA1
-IR
+IR
B
Vector:
empty
RNF168
HeLa + siRNF8 + IR
siRNA:
CTRL
RNF8
% rescue
Vector:
empty
empty
RNF168
C
RNF168
RNF168 C19S
UBC13
UEV1A
H2A
Ub(n)
Ub(2)
Ub(1)
blot: uH2A
H2B
blot: uH2B
blot: H2B
D
siCTRL
siRNF168
IR
Ub(2)
Ub(1)
blot: H2A (high exposure)
blot: H2A (low exposure)
blot: RNF168
E
ATM
DSB
MRN
HX
H2A
MDC1
RNF8
UBC13
Ubiquitin
RNF168
K63
53BP1
RAP80
ABRA1
BRCA1

postdoctoral fellow. D.D. is the Thomas Kierans Chair in Mechanisms of Cancer Development and a Canada Research Chair (Tier 2) in Proteomics, Bioinformatics, and Functional Genomics. This work was supported by CIHR grants (MOP84297 and MOP89754) to D.D.

Received: July 8, 2008
Revised: October 28, 2008
Accepted: December 22, 2008
Published: February 5, 2009

REFERENCES

Bekker-Jensen, S., Lukas, C., Kitagawa, R., Melander, F., Kastan, M.B., Bartek, J., and Lukas, J. (2006). Spatial organization of the Mamm. Genome surveillance machinery in response to DNA strand breaks. J. Cell Biol. *173*, 195–206.

Botuyan, M.V., Lee, J., Ward, I.M., Kim, J.E., Thompson, J.R., Chen, J., and Mer, G. (2006). Structural basis for the methylation state-specific recognition of histone H4-K20 by 53BP1 and Crb2 in DNA repair. Cell *127*, 1361–1373.

Callen, E., Nussenzweig, M.C., and Nussenzweig, A. (2007). Breaking down cell cycle checkpoints and DNA repair during antigen receptor gene assembly. Oncogene *26*, 7759–7764.

Difilippantonio, S., Gapud, E., Wong, N., Huang, C.Y., Mahowald, G., Chen, H.T., Kruhlak, M.J., Callen, E., Livak, F., Nussenzweig, M.C., et al. (2008). 53BP1 facilitates long-range DNA end-joining during V(D)J recombination. Nature *456*, 529–533.

DiTullio, R.A., Jr., Mochan, T.A., Venere, M., Bartkova, J., Sehested, M., Bartek, J., and Halazonetis, T.D. (2002). 53BP1 functions in an ATM-dependent checkpoint pathway that is constitutively activated in human cancer. Nat. Cell Biol. *4*, 998–1002.

Doil, C., Mailand, N., Bekker-Jensen, S., Menard, P., Larsen, D.H., Pepperkok, R., Ellenberg, J., Panier, S., Durocher, D., Bartek, J., et al. (2009). RNF168 binds and amplifies ubiquitin conjugates on damaged chromosomes to allow accumulation of repair proteins. Cell *136*, this issue, 435–446.

Huen, M.S., Grant, R., Manke, I., Minn, K., Yu, X., Yaffe, M.B., and Chen, J. (2007). RNF8 transduces the DNA-damage signal via histone ubiquitylation and checkpoint protein assembly. Cell *131*, 901–914.

Huyen, Y., Zgheib, O., Ditullio, R.A., Jr., Gorgoulis, V.G., Zacharatos, P., Petty, T.J., Sheston, E.A., Mellert, H.S., Stavridi, E.S., and Halazonetis, T.D. (2004). Methylated lysine 79 of histone H3 targets 53BP1 to DNA double-strand breaks. Nature *432*, 406–411.

Jacquemont, C., and Taniguchi, T. (2007). Proteasome function is required for DNA damage response and fanconi anemia pathway activation. Cancer Res. *67*, 7395–7405.

Jeggo, P.A., and Lobrich, M. (2007). DNA double-strand breaks: Their cellular and clinical impact? Oncogene *26*, 7717–7719.

Kittler, R., Heninger, A.K., Franke, K., Habermann, B., and Buchholz, F. (2005). Production of endoribonuclease-prepared short interfering RNAs for gene silencing in mammalian cells. Nat. Methods *2*, 779–784.

Kolas, N.K., Chapman, J.R., Nakada, S., Ylanko, J., Chahwan, R., Sweeney, F.D., Panier, S., Mendez, M., Wildenhain, J., Thomson, T.M., et al. (2007). Orchestration of the DNA-damage response by the RNF8 ubiquitin ligase. Science *318*, 1637–1640.

Lavin, M.F., and Shiloh, Y. (1997). The genetic defect in ataxia-telangiectasia. Annu. Rev. Immunol. *15*, 177–202.

Lou, Z., Minter-Dykhouse, K., Franco, S., Gostissa, M., Rivera, M.A., Celeste, A., Manis, J.P., van Deursen, J., Nussenzweig, A., Paull, T.T., et al. (2006). MDC1 maintains genomic stability by participating in the amplification of ATM-dependent DNA damage signals. Mol. Cell *21*, 187–200.

Mailand, N., Bekker-Jensen, S., Faustrup, H., Melander, F., Bartek, J., Lukas, C., and Lukas, J. (2007). RNF8 ubiquitylates histones at DNA double-strand breaks and promotes assembly of repair proteins. Cell *131*, 887–900.

Manis, J.P., Morales, J.C., Xia, Z., Kutok, J.L., Alt, F.W., and Carpenter, P.B. (2004). 53BP1 links DNA damage-response pathways to immunoglobulin heavy chain class-switch recombination. Nat. Immunol. *5*, 481–487.

Matsuoka, S., Ballif, B.A., Smogorzewska, A., McDonald, E.R., III, Hurov, K.E., Luo, J., Bakalarski, C.E., Zhao, Z., Solimini, N., Lerenthal, Y., et al. (2007). ATM and ATR substrate analysis reveals extensive protein networks responsive to DNA damage. Science *316*, 1160–1166.

McKinnon, P.J., and Caldecott, K.W. (2007). DNA strand break repair and human genetic disease. Annu. Rev. Genomics Hum. Genet. *8*, 37–55.

Newton, K., Matsumoto, M.L., Wertz, I.E., Kirkpatrick, D.S., Lill, J.R., Tan, J., Dugger, D., Gordon, N., Sidhu, S.S., Fellouse, F.A., et al. (2008). Ubiquitin chain editing revealed by polyubiquitin linkage-specific antibodies. Cell *134*, 668–678.

Nicassio, F., Corrado, N., Vissers, J.H., Areces, L.B., Bergink, S., Marteijn, J.A., Geverts, B., Houtsmuller, A.B., Vermeulen, W., Di Fiore, P.P., and Citterio, E. (2007). Human USP3 is a chromatin modifier required for S phase progression and genome stability. Curr. Biol. *17*, 1972–1977.

Penengo, L., Mapelli, M., Murachelli, A.G., Confalonieri, S., Magri, L., Musacchio, A., Di Fiore, P.P., Polo, S., and Schneider, T.R. (2006). Crystal structure of the ubiquitin binding domains of rabex-5 reveals two modes of interaction with ubiquitin. Cell *124*, 1183–1195.

Plans, V., Scheper, J., Soler, M., Loukili, N., Okano, Y., and Thomson, T.M. (2006). The RING finger protein RNF8 recruits UBC13 for lysine 63-based self polyubiquitylation. J. Cell. Biochem. *97*, 572–582.

Figure 7. RNF168 Ubiquitylates H2A

(A) U2OS cells transfected either with control (siCTRL) or the indicated siRNAs were irradiated with a 10 Gy dose. At 4 hr after irradiation, cells were fixed and processed for ubiquitylated H2A (uH2A) and γ-H2AX immunofluorescence. Controls for the effectiveness of the siRNAs can be found in Figure S8. DNA was counterstained with DAPI. (Lower panel) Quantitation of uH2A foci. Data are represented as the mean ± SD (n = 3).

(B) HeLa cells were transfected first with either nontargeting control (CTRL) or RNF8 (RNF8) siRNAs. After transfection, cells were reseeded and transfected either with an empty control vector (empty) or wild-type RNF168. At 24 hr after plasmid transfections, cells were irradiated with a 10 Gy dose and fixed 1 hr postirradiation to be processed for 53BP1 immunofluorescence. DNA was counterstained with DAPI. (Upper panel) Representative micrographs. (Bottom graph) Quantitation of 53BP1 foci from the experiment. Data are represented as the mean ± SD (n = 3). Control immunoblots are shown in Figure S5D.

(C) Ubiquitylation assays employing the indicated GST-RNF168 proteins were assembled with either H2A (upper panel) or H2B (lower panel) as substrates. The reaction products were analyzed by immunoblotting with the ubiquitylated H2A (uH2A) or H2B (uH2B) antibodies. Total H2B was also monitored for input.

(D) HeLa cells were first transfected with control (siCTRL) or RNF168 (siRNF168) siRNAs. At 36 hr after transfection, cells were irradiated with a 10 Gy dose and harvested 1 hr after irradiation. Histones were isolated by acid extraction and separated by SDS-PAGE and blotted with an anti-H2A antibody. (Upper panel) An exposure that examines the ubiquitylated H2A species. (Lower panel) A lower exposure of the same blot showing the unmodified H2A band.

(E) Model of RNF168 action at sites of DNA damage. Following recognition of a DNA double-strand break (DSB) by the MRN complex, MDC1 is recruited to the surrounding chromatin by binding to γ-H2AX (HX), whereby it is phosphorylated on "TQXF" motifs by ATM. RNF8-UBC13 binds to phospho-MDC1 and ubiquitylates histones H2A and H2AX. uH2A promotes recruitment of the RNF168-UBC13 complex, which, in turn, amplifies H2A ubiquitylation. RNF168 likely ubiquitylates other, as-yet unidentified, chromatin-bound substrate(s) (denoted by "?"). The ubiquitylation of various histones and other chromatin-bound proteins surrounding the DNA break mediates the recruitment of RAP80-ABRA1-BRCA1 complex via the ubiquitin-interacting domains (UIM) of RAP80. 53BP1 relocalization to sites of damage is aided by the recognition of methylated histones by its Tudor domain.

Rogakou, E.P., Pilch, D.R., Orr, A.H., Ivanova, V.S., and Bonner, W.M. (1998). DNA double-stranded breaks induce histone H2AX phosphorylation on serine 139. J. Biol. Chem. *273*, 5858–5868.

Sakasai, R., and Tibbetts, R. (2008). RNF8-dependent and RNF8-independent regulation of 53BP1 in response to DNA damage. J. Biol. Chem. *283*, 13549–13555.

Savitsky, K., Barshira, A., Gilad, S., Rotman, G., Ziv, Y., Vanagaite, L., Tagle, D.A., Smith, S., Uziel, T., Sfez, S., et al. (1995). A single ataxia telangiectasia gene with a product similar to Pi 3 kinase. Science *268*, 1749–1753.

Sobhian, B., Shao, G., Lilli, D.R., Culhane, A.C., Moreau, L.A., Xia, B., Livingston, D.M., and Greenberg, R.A. (2007). RAP80 targets BRCA1 to specific ubiquitin structures at DNA damage sites. Science *316*, 1198–1202.

Stewart, G.S., Wang, B., Bignell, C.R., Taylor, A.M., and Elledge, S.J. (2003). MDC1 is a mediator of the mammalian DNA damage checkpoint. Nature *421*, 961–966.

Stewart, G.S., Stankovic, T., Byrd, P.J., Wechsler, T., Miller, E.S., Huissoon, A., Drayson, M.T., West, S.C., Elledge, S.J., and Taylor, A.M. (2007). RIDDLE immunodeficiency syndrome is linked to defects in 53BP1-mediated DNA damage signaling. Proc. Natl. Acad. Sci. USA *104*, 16910–16915.

Stiff, T., O'Driscoll, M., Rief, N., Iwabuchi, K., Lobrich, M., and Jeggo, P.A. (2004). ATM and DNA-PK function redundantly to phosphorylate H2AX after exposure to ionizing radiation. Cancer Res. *64*, 2390–2396.

Stucki, M., Clapperton, J.A., Mohammad, D., Yaffe, M.B., Smerdon, S.J., and Jackson, S.P. (2005). MDC1 directly binds phosphorylated histone H2AX to regulate cellular responses to DNA double-strand breaks. Cell *123*, 1213–1226.

Wang, B., and Elledge, S.J. (2007). Ubc13/Rnf8 ubiquitin ligases control foci formation of the Rap80/Abraxas/Brca1/Brcc36 complex in response to DNA damage. Proc. Natl. Acad. Sci. USA *104*, 20759–20763.

Wang, B., Matsuoka, S., Carpenter, P.B., and Elledge, S.J. (2002). 53BP1, a mediator of the DNA damage checkpoint. Science *298*, 1435–1438.

Wang, H., Wang, L., Erdjument-Bromage, H., Vidal, M., Tempst, P., Jones, R.S., and Zhang, Y. (2004). Role of histone H2A ubiquitination in Polycomb silencing. Nature *431*, 873–878.

Zhu, B., Zheng, Y., Pham, A.D., Mandal, S.S., Erdjument-Bromage, H., Tempst, P., and Reinberg, D. (2005). Monoubiquitination of human histone H2B: The factors involved and their roles in HOX gene regulation. Mol. Cell *20*, 601–611.